ADVENGMAT
ISSN 1438-1656
Vol. 17 – No. 3
March, 2015

ADVANCED ENGINEERING MATERIALS

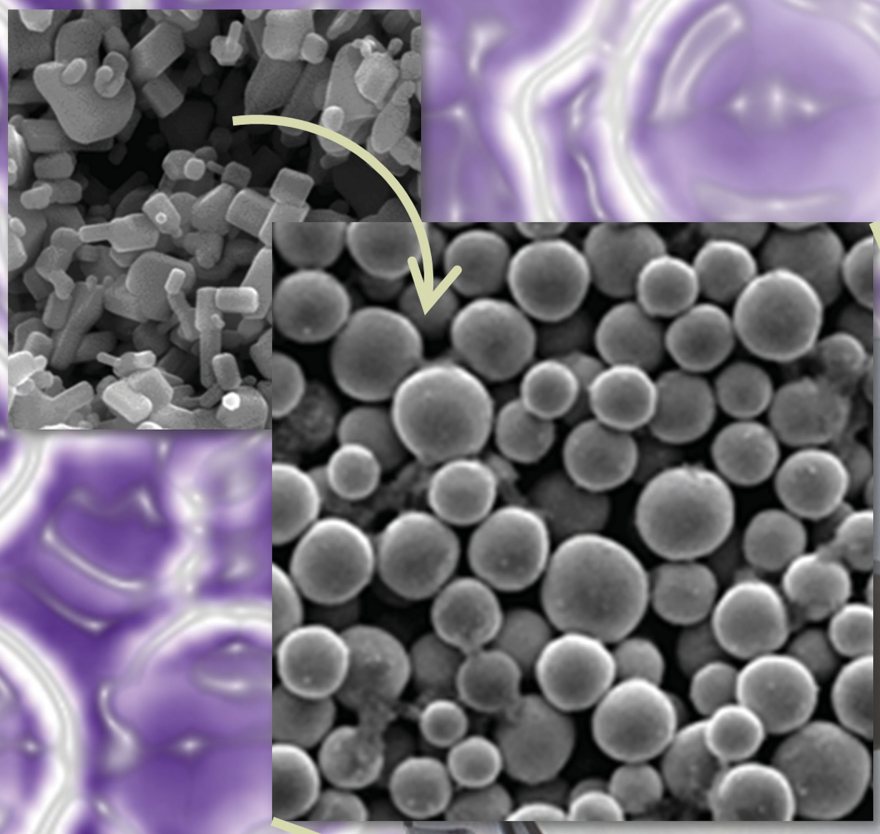

WILEY-VCH

ADVANCED ENGINEERING MATERIALS

DOI: 10.1002/adem.201400385

Morphology Evolution of ZnO Submicroparticles Induced by Laser Irradiation and Their Enhanced Tribology Properties by Compositing with Al_2O_3 Nanoparticles**

By *Guangbin Duan, Xilun Hu, Xiaoyun Song, Zhiwen Qiu, Haibo Gong* and *Bingqiang Cao**

In this paper, ZnO submicrospheres are prepared by a simple laser-stimulated surface tension energy release strategy, which is a very convenient method for growing inorganic oxide spheres with high melting points. The detailed morphology evolution of ZnO particles is investigated by changing the laser fluence. The formation of spherical morphology is due to the particle spherizing and/or coalescence as a result of surface area minimum and release of surface tension energy when particles are heated by laser irradiation. ZnO submicrospheres can effectively reduce the friction coefficients when used as lubricating oil additives, which exhibit a clear morphology-dependent property. But the wear becomes worse due to its small hardness. However, the compositing ZnO submicrospheres with Al_2O_3 nanoparticles as the lubricating oil additives can notably improve both the friction-reduction and anti-wear properties. The surface analysis of the thrust rings suggests that rolling friction becomes dominant instead of sliding friction and these composite particles squeezed into the grooves on the rubbing surfaces can reduce wear.

1. Introduction

Preparation and application of nanoparticles have attracted much attention due to their unique optical[1,2] and electrical[3,4] properties in recent years. It is also worth noting that, with the size and shape-dependent mechanical property, nanoparticles have also shown good potential as lubricant and/or their additives for tribology applications.[5–7] However, in this case, how to synthesis nanoparticles with special size and morphology is very important. Generally speaking, there are two kinds of methods to prepare nanoparticles, e.g., physical and chemical methods, such as sol–gel,[8] hydrothermal method,[9] chemical bath deposition,[10] and laser ablation.[11] But nanoparticles with relative high surface activity prepared by these methods are easy to agglomerate and hard to disperse without modifications. Therefore, these disadvantages limit their tribology application.

Recently, laser ablation has been adopted to synthesize particles both in vapor or liquid medium, which is known as pulsed laser ablation (PLA). The PLA synthesis of nanomaterials in a vacuum or gaseous environment is usually combined with a tube furnace and also known as laser-assisted chemical vapor deposition[12] or high-pressure pulsed laser deposition.[13] The combination of laser ablation and vapor transport deposition provide good control over the temperature, pressure, and gas follow to grow nanostructures, especially for one-dimensional nanowires or two-dimensional nanowalls.[14,15] Laser ablation in liquid (LAL) media was firstly implemented to fabricate colloidal solution of nanoparticles, known as LAL.[16,17] When the solid target is

[*] *Prof. B. Cao, Dr. G. Duan, X. Hu, X. Song, Z. Qiu, Dr. H. Gong*
Key Laboratory of Functional Inorganic Materials in Universities of Shandong, School of Material Science and Engineering, University of Jinan, Jinan 250022, China
Prof. B. Cao
Shandong Provincial Key Laboratory of Preparation and Measurement of Building Materials, University of Jinan, Jinan 250022, Shandong, China
E-mail: mse_caobq@ujn.edu.cn

[**] *This work is supported by NSFC (11174112, 51472110) and Shandong Provincial Science Foundation for Disguised Youth Scholars (JQ201214). The research programs from Ministry of Education, China, are also acknowledged (NCET-11-1027, 213021A). B. C. thanks the Taishan Scholar Professorship (TSHW20091007) tenured at University of Jinan.*
Supporting Information is available online from Wiley Online Library or from the author.

irradiated in liquid, due to the extreme non-equilibrium conditions generated by laser, the surface of the solid target vaporizes and reassembles to colloidal nanoparticles.[18,19] For example, Yang *et al.*[20] synthesized Si quantum dots using PLA in liquid method and anomalous quantum confinement effect was observed. If simply irradiating well-dispersed powder particles in liquid instead of solid target, the application of laser with proper energy makes the change of particle morphology possible.[21] Koshizaki and coworkers[22] have prepared metal and semiconductor submicrometer spheres by a selective pulsed heating with visible laser.

In view of the basic principles of lubricant, spherical particles with big hardness can be expected to change sliding friction into rolling friction more effectively and reduce the wear more significantly in comparison with other shaped particles (e.g., faceted particles), which are considered to be highly favorable in tribological applications. Unfortunately, syntheses of inorganic crystalline spheres have rarely been reported, possibly because of their very high melting points and anisotropic crystal structures. We have synthesized a series of submicrometer scale spherical metal oxide particles and its tribological properties as lubricating additives were also primary evaluated.[23] These oxide spherical particles like ZnO, TiO_2, or Cu_2O perform excellent friction-reduction properties. However, due to its low hardness, the anti-wear property is needed to be improved. Herein, we first investigated the morphology evolution of ZnO particles under laser irradiation in water. Then these raw ZnO particles and as-prepared submicrospheres were compared as lubricating oil additives and exhibited a clear morphology-related friction-reduction property. Moreover, by compositing with Al_2O_3 nanoparticles, such ZnO submicrospheres also exhibited effective anti-wear properties.

2. Experimental Section

ZnO submicrometer spheres were prepared by irradiating raw commercial ZnO powders (99.999%, Sigma) for 30 min dispersed in a quatz cell with a diameter of 3 cm. Pure distilled water (Ph = 7) was used as solvent to form a ZnO suspension (0.2 mg mL^{-1}). Usually, the water cell was half filed with the above ZnO suspension and kept at room temperature. Average size of raw ZnO powder was below 1.0 μm. The wavelength of pulsed KrF excimer laser is 248 nm (10 Hz, 25 ns, Coherent, CompexPro 205). The laser energy density can be tuned from 0.1 to 2.5 J $pulse^{-1}$ cm^{-2}, which was monitored with a FieldMaxII-TOP laser energy meter (Coherent). All of the prepared suspensions were centrifuged at 12 000 rpm after laser irradiation and then dried at 50 °C for further characterizations and applications. Al_2O_3 nanoparticles were prepared by hydrothermal method according to our previous report.[24]

Phase and morphology analyses were carried out by X-ray diffraction (XRD) measurements using an X-ray diffractometer (D8-ADVANCE, Bruker) with Bragg–Brentano geometry using Cu Kα radiation and field emission scanning electron microscope (FESEM; Quanta FEG). Transmission electron microscope (TEM; JEM-2010, JEOL) was used to observe the microstructure of the prepared samples. The tribological properties of the prepared ZnO and ZnO/Al_2O_3 particles as lubricating oil additives were investigated by thrust-ring and four-ball tests (MMU-10G, Sinomach-Jinan) in terms of friction coefficient and wear scar diameter (WSD). Samples with different concentration of such particles were tested carefully and detailed experimental condition was shown in Table 1.

3. Results and Discussion

3.1. General Morphology Evolution of ZnO Particles under Laser Irradiation

Figure 1 shows the XRD patterns of raw ZnO powder and as-prepared ZnO samples after laser irradiation under fluence of 0.4 J $pulse^{-1}$ cm^{-2}. All diffraction peaks from both two samples can be identified as pure ZnO of wurtzite structure (JCPDS 36-1415). It indicates the application of laser irradiation in preparing ZnO spherical particles have not introduced new phases.

Figure 2 compares the morphology of the raw commercial and irradiated ZnO particles. Figure 2a is the SEM image of raw irregular rod-like particles that is a typical shape of solution-grown ZnO powders due to its anisotropic hexagonal crystal structure. While, after laser irradiation, the ZnO particles are perfect spheres with smooth surfaces, as shown in Figure 2b. Figure 2c compares the particle size distribution of raw ZnO particles and as-prepared ZnO spheres. From Figure 2c, we can see the average size of as-prepared ZnO spheres is mainly between 400 and 800 nm. We measured the diameters of 200 raw commercial ZnO particles and estimated the average size was about 400 nm, as indicated with the dashed column in Figure 2c. This indicates that, when raw ZnO particles were irradiated with laser, the average size of ZnO particles become a little larger compared with that of raw ZnO powders.

Table 1. Experimental parameters of thrust-ring and four-ball tests.

Test	Orbiting speed [r min^{-1}]	Load [N]	Temperature [K]	Operating time [s]
Thrust-ring test	1200	200	348	1800
Four-ball test	1450	147	348	1800

ADVANCED ENGINEERING MATERIALS

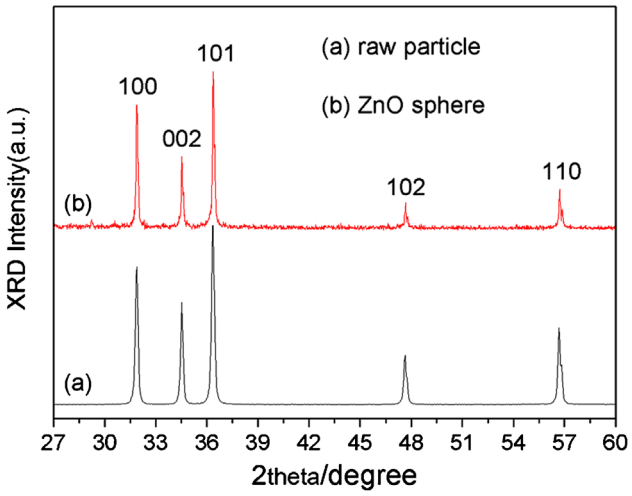

Fig. 1. XRD patterns of ZnO particles. (a) Raw ZnO powders, (b) ZnO submicrometer spheres irradiated with laser of 0.4 J pulse^{-1} cm^{-2}.

Figure 3 shows the SEM images of prepared ZnO particles irradiated with laser of different energy density. When the laser energy density is below 100 mJ pulse^{-1} cm^{-2}, it cannot produce enough thermal energy through irradiation to melt all the particles and only a few smaller particles change to spheres (Figure 3b). With increasing laser fluence, most particles melt and show different morphologies from the original ones and their surfaces begin to shrink. Few smaller particles already exhibit spherical morphology (Figure 3c). ZnO particles then change to ideal spheres when laser energy density is 0.4 J pulse^{-1} cm^{-2}, as shown in Figure 3d. A closer look finds that many small particles are swallowed by larger ones and Figure 3e typically illustrates the particles merging process. During this process, the total volume of all particles keep constant while surface area is reduced, and, therefore,

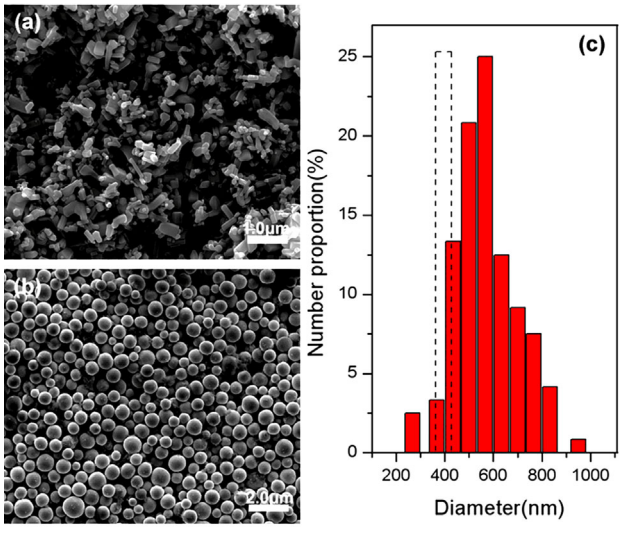

Fig. 2. SEM images of ZnO particles. (a) Raw ZnO particles, (b) ZnO submicrometer spheres obtained by pulsed laser irradiation (0.4 J pulse^{-1} cm^{-2}), (c) Particle size distribution of prepared ZnO submicrometer spheres. The dashed column indicated the estimated average size of raw particles.

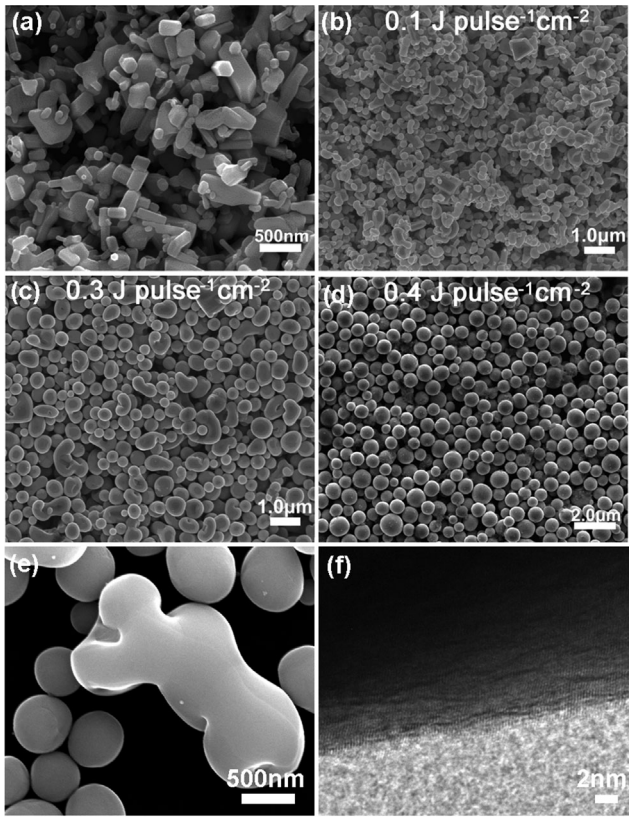

Fig. 3. (a–d) SEM images of ZnO particles prepared by irradiation of commercial ZnO powders with different laser fluence. The laser frequency and irradiation time were 10 Hz and 30 min. (e) A typical particle from (c), (f) a high-resolution TEM image of a ZnO submicrosphere edge.

the surface energy of particles also decreases. As we all know, spherical particles enclosing a given volume with low surface energy are most stable. This physical growth process can simply described as a laser-stimulated surface tension energy release (LSSTER) method. More discussion about the ZnO, TiO_2, CuO, and Fe_3O_4 spheres growth through LSSTER method can be found in our former paper.[23,24] Typical high-resolution TEM image shown in Figure 3f proves these ZnO spheres after laser irradiation are of single crystal with clean surface, which is also consisted with the former results of Wang *et al.*[22]

But when the laser energy density continues to increase to 1000 mJ pulse^{-1} cm^{-2}, besides bigger ZnO spheres, some much smaller nanoparticles with diameter of several nanometers appear (Figure 4a and b). The generation of such nanoparticles is a typical chemical process that was called LAL.[16,17] High-energy density laser creates local high-temperature and high-pressure plasma plumes above the target surface, e.g., ZnO powders in water here. Such plasma plume was reported to form in about 60 ns after the interaction between the laser and target, and its temperature was up to 6000 K and started to decrease in about 1000 ns.[25] During this transient process, the laser ablated gaseous substance fast reassemble to form nanoparticles. So, such particles are usually very small, which is a typical difference to the submicrospheres formed by the above physical LSSTER

FULL PAPER

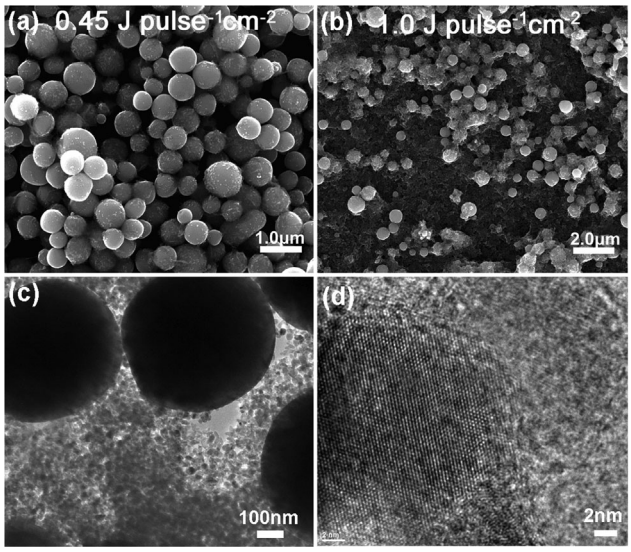

Fig. 4. (a and b) SEM images of ZnO particles obtained by laser irradiation with energy density of 0.45 and 1 J pulse^{-1} cm^{-2}. The laser frequency and irradiation time were 10 Hz and 30 min. (c) TEM image of corresponding ZnO submicrospheres and nanoparticles, (d) a HRTEM image of a small ZnO nanoparticles shown in (c).

process. From the corresponding TEM images in Figure 4c and d, the particle size difference were more clearly seen. Moreover, high-resolution TEM image (Figure 4d) indicates smaller ZnO particles are also of single crystal.

3.2. Tribology Properties of Submicrospheres as Lubricating Additives

3.2.1. Frication-Reduction Property of ZnO Submicrospheres

As we know, nanoparticles as lubricating oil additives usually need to be surface modified to prevent the agglomeration caused by their polar and hydrophilic surfaces.[26,27] The ZnO submicrometer spheres prepared by the simple LSSTER method showed good dispersibility in commercial lubricating oil without any surface modification, as shown in Supporting Information Figure S1. Even after 30 days, the suspensions are still turbid with high haze, which indicates the ZnO/lubricating oil solution is still homogenous and stable. So, this property is benefit for its further application as lubricating oil additives.

To study the morphology-related application of such ideal spherical particles, friction properties were first investigated by using the prepared ZnO submicrometer spheres (0.4 J pulse^{-1} cm^{-2}) as lubricating oil additives. Figure 5 shows the friction coefficient curves measured by thrust-ring test. We can see that when raw ZnO particles with irregular morphology were added into the oil, the friction coefficient (Figure 5b) increases clearly in comparison with pristine lubricating oil (Figure 5a). But when ZnO submicrometer spheres were added into the oil, the friction coefficients all decreases obviously. Moreover, the friction-reduction properties show a clear dependence on the concentration of the added ZnO spherical particles. The optimal concentration of ZnO additives was 0.10 wt% (Figure 5e), and the average friction coefficient of Sample (e) was 0.01767 with a reduction of 62.0% compared to Sample (a), that is, blank oil with a friction coefficient of 0.04647. However, the friction coefficient increased when the concentration of ZnO spheres in lubricating oil was more than 0.10 wt% (Samples f and g). This illustrated that superfluous ZnO spheres in oil were not needed to reduce the friction. The friction-reduction effect was summarized in Supporting Information Table S1. This can be

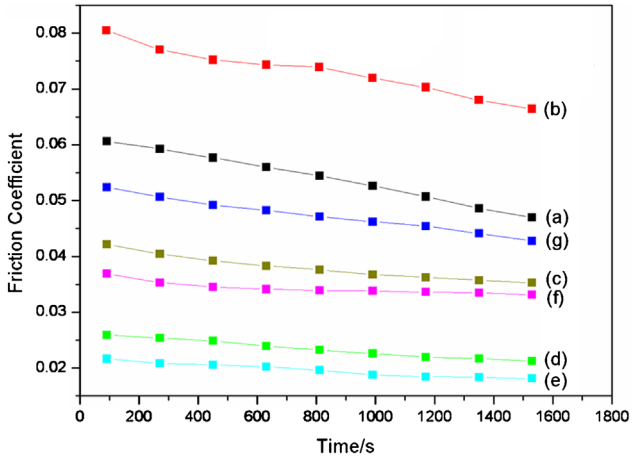

Fig. 5. Friction coefficient curves of thrust-ring test. (a) Pristine lubricating oil, (b) lubricating oil with 0.03 wt% raw ZnO particles, (c–g) lubricating oil with ZnO submicrospheres of different concentration. Curves (a–g) correspond to Samples (a–g) in Table 2, respectively.

Table 2. Friction coefficients measured by four ball test when ZnO and ZnO/Al_2O_3 were added into lubricating oil in comparison with commercial oil.

Additives	Sample	Concentration x/wt%	Averaged fiction coefficient	Friction change [+/−%]	WSD [μm]	WSD change [+/−%]
ZnO	a	0	0.07143	–	296.56	–
	b	0.05	0.05632	−21.15	316.32	+6.66
	c	0.10	0.03848	−46.13	317.16	+6.95
	d	0.15	0.06205	−13.13	314.46	+6.04
	e	0.20	0.07627	+6.78	319.97	+7.89
ZnO/Al_2O_3	A	0/0	0.07300	–	309.17	–
	B	0.1/0	0.03547	−51.41	337.23	+9.06
	C	0.1/0.05	0.02917	−60.04	290.38	−6.08
	D	0.1/0.10	0.03984	−45.42	234.23	−24.24
	E	0.1/0.15	0.06115	−16.23	257.17	−17.47

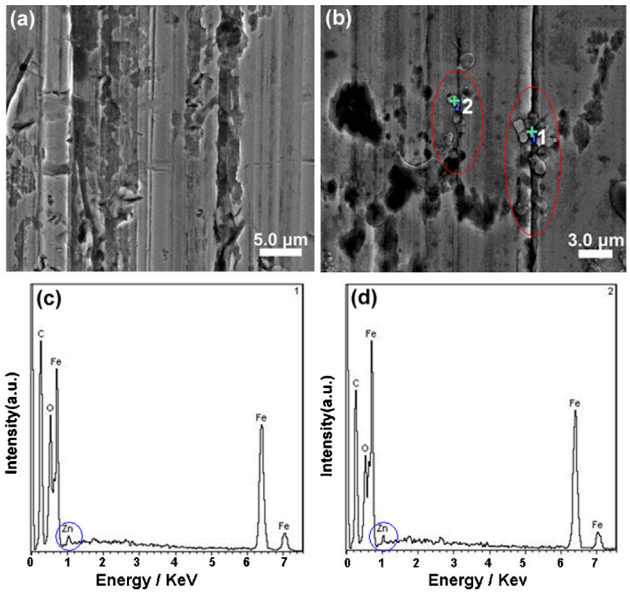

Fig. 6. SEM and EDS images of wear surface after thrust ring test. (a) Blank lubricating oil, (b) after added ZnO spheres, (c, d) are EDS images of two dots in (b), respectively.

basically attributed to the rolling friction effect that the regular spherical ZnO micrometers can act as molecular bearing between two rubbing surfaces.[28] Therefore, the influence of ZnO sphere concentration on their friction performance can be understood.

However, so far, the exact mechanism of micro/nanoparticle lubricating additives to decrease friction is still not clear.[29,30] But inorganic particles as lubricating oil additives possess the features of serving as spacer, e.g., molecular bearing for rolling friction, and forming a lubrication film.[31,32] Also, micro/nanoparticles deposited on the grooves of friction surface can compensate the loss of mass, which is called as the mending effect.[33] To understand the lubricating mechanism, SEM and EDS were further adopted to check the wear surface after thrust-ring test, as shown in Figure 6. There are many grooves and valleys on the wear surface after thrust-ring test using pristine oil, see Figure 6a. But when ZnO spheres were added into lubricating oil, the wear surface become smooth and some particles are squeezed into the grooves on the wear surface (Figure 6b), as indicated by red circles. EDS spectra of Regions 1 and 2 illustrate the ZnO spheres compensate the loss of mass, and this is consistent with the reported mending effect.[34]

3.2.2. Improve Anti-Wear Property of ZnO Submicrospheres by Compositing with Al_2O_3 Nanoparticles

Besides friction reduction effect, anti-wear property is an equally important characteristic for lubricating oil applications. Figure 7 shows the morphology and WSD of testing balls when ZnO submicrospheres of different concentrations were added into lubricating oil. The dependence of friction coefficients on the concentrations of ZnO spheres measured with four-ball test

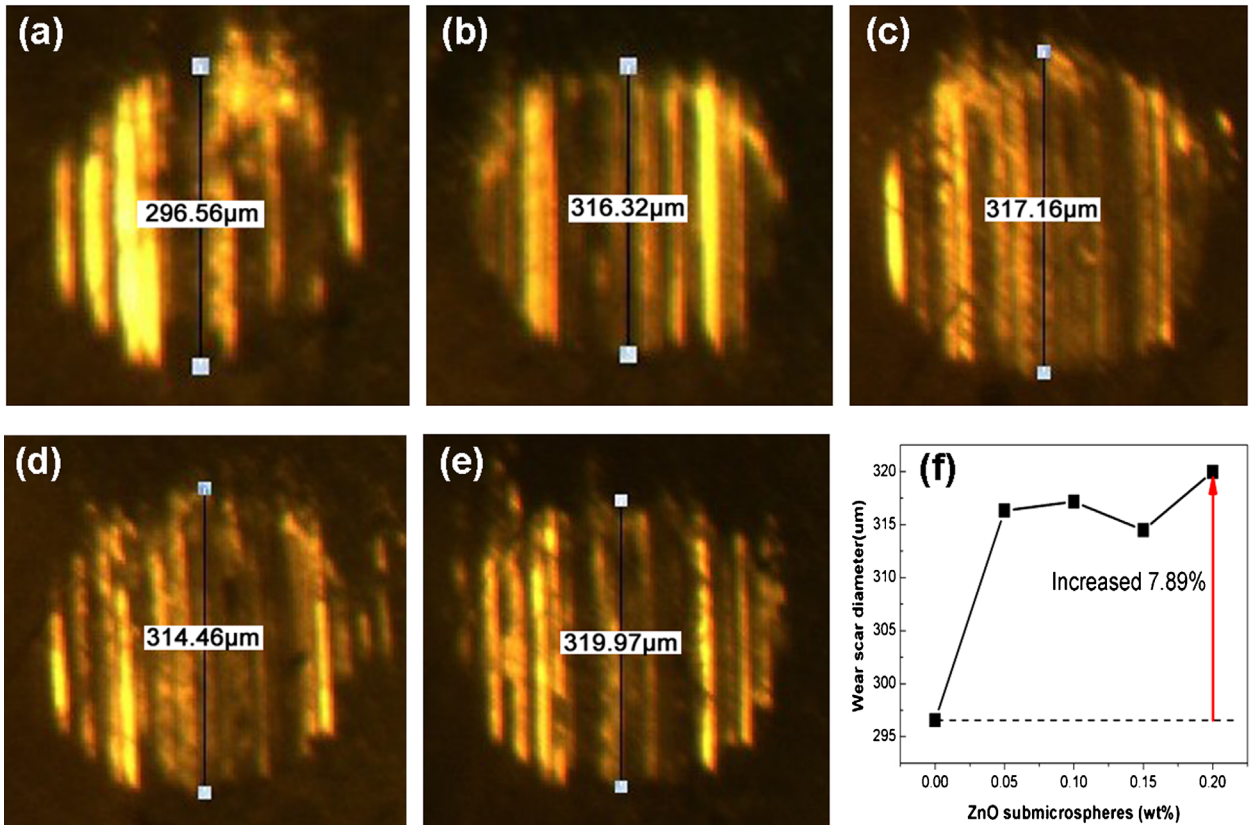

Fig. 7. (a–e) Morphology and size of WSD when ZnO spheres of different concentration were added into lubricating oil measured with four-ball test. Image (a–e) corresponds to Samples (a–e) summarized in Table 3, respectively. (f) WSD size comparison.

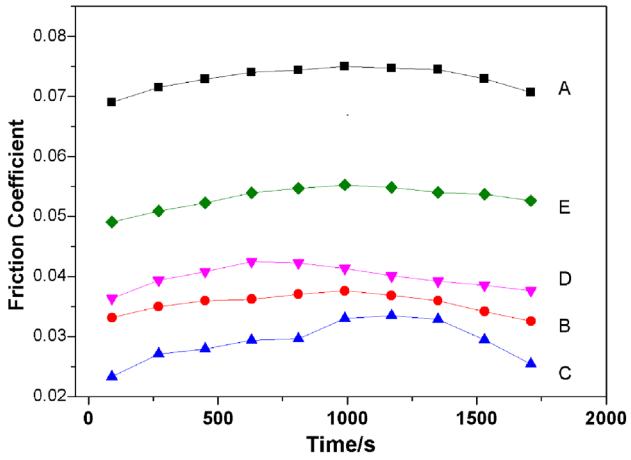

Fig. 8. Friction coefficient versus time when ZnO/Al_2O_3 composite particles were added into lubricating oil measured with four-ball test method. Curve (A–E) corresponding to Samples (A–E) summarized in Table 3.

method exhibits similar behavior (not shown here) to that measured by thrust-ring method. However, the WSD only increased when the ZnO spheres were added, although the friction coefficient was decreased clearly. This means the addition of ZnO submicrospheres causes more severe wear. Clearly, it is not desired for practical applications.

ZnO is a relatively soft material with approximate hardness of 4.5 on the Mohs scale, while Al_2O_3 is relatively hard (≈9 Ms). Therefore, based on above and our former experimental results,[35,36] ZnO/Al_2O_3 composite particles would be expected to demonstrate better tribology properties in terms of both friction reduction and anti-wear. When the concentration of ZnO spheres was 0.01 wt%, the friction-reduction effect was best according to above experimental results in thrust-ring test (Figure 5). So, in order to keep the optimal friction-reduction effect, we fixed the concentration of ZnO spheres at 0.01 wt%, and simultaneously added our formerly hydrothermal grown Al_2O_3 nanoparticles[37,38] of different concentration to study their friction and wear properties. Controlled experimental design was shown in Table 2. Figures 8 and 9 show the friction coefficient curves versus time and WSD images, respectively, when ZnO/Al_2O_3 composite particles were added into the lubricating oil measured with four-ball test method. We can see from Figure 9 that the friction coefficients were further decreased when Al_2O_3 nanoparticles were added and the optimal Al_2O_3 concentration is 0.05 wt% (Sample C in Table 2).

For anti-wear property of this series of Samples A–E, when only ZnO spheres (0.1 wt%) were added into lubricating oil, the WSD increased from 309.17 μm of pristine oil to 337.23 μm (Figure 9a and b). However, the WSD decreased to 290.38 μm significantly when additional Al_2O_3 nanoparticles (0.05 wt%, Figure 9c) were added. Moreover, the WSD further decreased while the friction coefficients increased slightly when the concentration of Al_2O_3 nanoparticles was bigger than

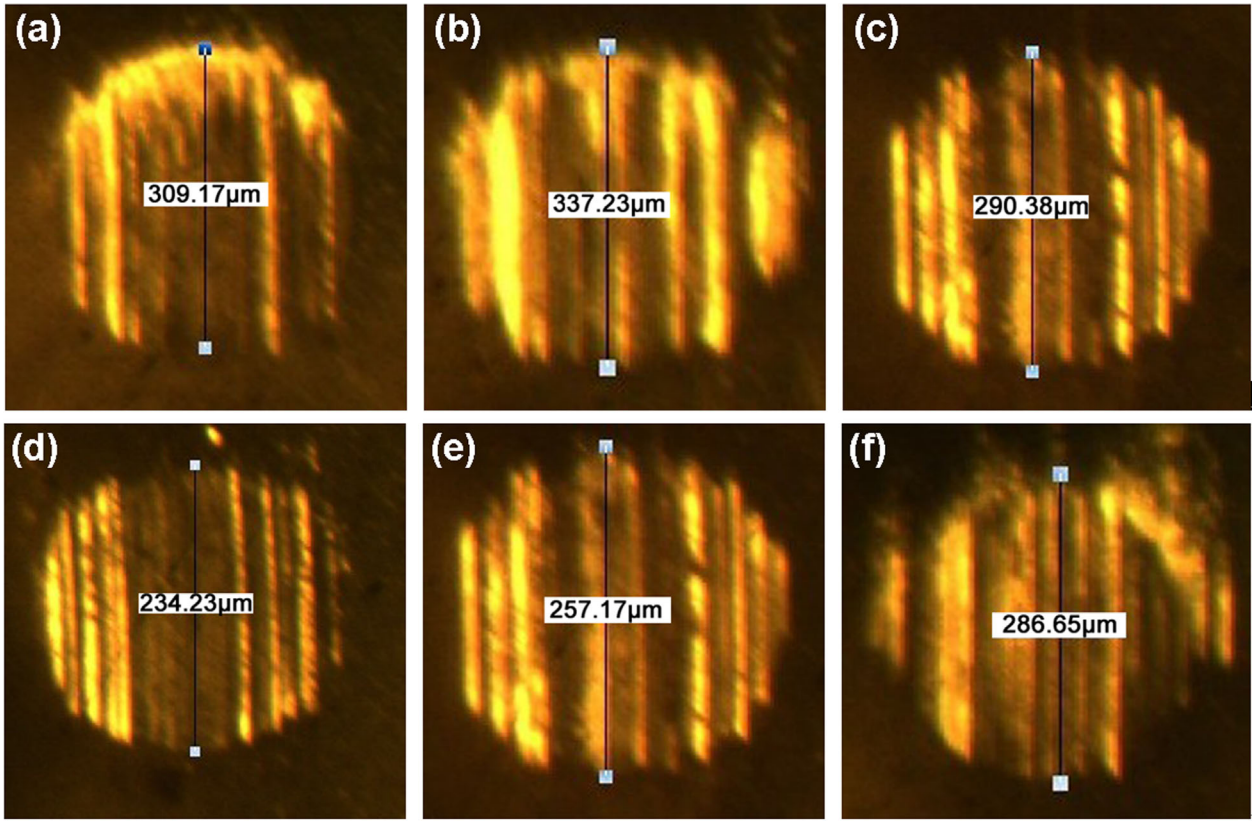

Fig. 9. Morphology and diameter of wear scar under different concentration of ZnO/Al_2O_3 in four-ball test. Images (a–f) corresponding to Samples (A–F) in Table 3.

0.05 wt%. The optimal concentration of Al_2O_3 nanoparticles for anti-wear property was 0.1 wt% (Sample D). In this case, the WSD decreased to 234.23 μm, but the reduction of friction coefficient was not as large as that of Sample C. Further increase of Al_2O_3 nanoparticles concentration (e.g., 0.15 wt%, Sample E) would increase both the friction coefficient and the WSD. Although the anti-wear effect of adding Al_2O_3 nanoparticles into lubricating oil is consistent with the former reports,[39,40] the integrated application of ZnO spheres and Al_2O_3 nanoparticles as lubricating additives to improve their tribological properties, e.g., friction-reduction and anti-wear, simultaneously, is more preferable for practical applications.

4. Conclusion

In conclusion, we demonstrated the growth of ideal ZnO submicrospheres with smooth surface by a simple LSSTER method and their application through compositing with Al_2O_3 nanoparticles for enhanced tribology properties. The morphology of ZnO particles grown with LSSTER method can be well controlled by laser fluence. This is the most convenient approach for fabricating inorganic oxide spherical particles with high melting point at present. The ZnO submicrospheres exhibit clear morphology-dependent friction reduction property but no anti-wear effect. However, the integrated application of ZnO submicrospheres and Al_2O_3 nanoparticles as the lubricating oil additives can notably improve both the friction-reduction and anti-wear properties. When ZnO/Al_2O_3 particles are added to lubricating oil, the friction coefficient and WSD are both decreased. The optimal concentration of ZnO/Al_2O_3 is 0.1/0.1 wt% and the WSD and friction coefficient decreased 24.2 and 45.4%, respectively, in comparison with pristine lubricating oil. This is mainly because rolling friction becomes dominant instead of sliding friction and these composite micro/nanoparticles squeezed into the grooves on the rubbing surfaces can reduce wear.

Received: August 18, 2014
Final Version: September 19, 2014
Published online: November 6, 2014

[1] K. L. Kelly, E. Coronado, L. L. Zhao, G. C. Schztz, *J. Phys. Chem. B* **2003**, *107*, 668.
[2] Y. Li, M. Ge, J. W. Li, J. F. Wang, H. J. Zhang, *Cryst. Eng. Commun.* **2011**, *13*, 637.
[3] X. L. Zhao, X. B. Ding, Z. H. Deng, Z. H. Zheng, Y. X. Peng, C. R. Tian, X. P. Long, *New. J. Chem.* **2006**, *30*, 915.
[4] C. Y. Huang, D. Y. Wang, C. H. Wang, Y. T. Chen, Y. T. Wang, Y. T. Jiang, Y. J. Yang, C. C. Chen, Y. F. Chen, *ACS Nano* **2010**, *4*, 5849.
[5] D. Guo, G. X. Xie, J. B. Luo, *J. Phys. D. Appl. Phys.* **2014**, *47*, 013001.
[6] M. Feldmann, D. Dietzel, H. Fuchs, A. Schirmeisen, *Phys. Rev. Lett.* **2014**, *112*, 155503.
[7] C. Drummond, N. Alcantar, J. Israelachvili, R. Tenne, Y. Golan, *Adv. Funct. Mater.* **2001**, *11*, 348.
[8] S. Lee, I. S. Cho, J. H. Lee, D. H. Kim, D. W. Kim, J. Y. Kim, H. Shin, J. K. Lee, H. S. Jung, N. G. Park, K. Kim, M. J. Ko, K. S. Hong, *Chem. Mater.* **2010**, *22*, 1958.
[9] A. A. Firooz, A. R. Mahjoub, A. A. Khodadadi, *Mater. Lett.* **2008**, *62*, 1789.
[10] C. T. Wu, W. P. Liao, J. J. Wu, *J. Mater. Chem.* **2011**, *21*, 2871.
[11] H. B. Zeng, W. P. Cai, Y. Li, J. L. Hu, P. S. Liu, *J. Phys. Chem. B* **2005**, *109*, 18260.
[12] Y. Shen, J. I. Hong, S. Xu, S. Lin, H. Fang, S. Zhang, Y. Ding, R. L. Snyder, Z. L. Wang, *Adv. Funct. Mater.* **2010**, *20*, 703.
[13] B. Q. Cao, M. Lorenz, A. Rahm, H. Von Wenckstern, C. Czekalla, J. Lenzner, G. Benndorf, M. Grundmann, *Nanotechnology* **2007**, *18*, 455707.
[14] Z. W. Qiu, X. P. Yang, J. Han, P. Zhang, B. Q. Cao, Z. F. Dai, G. T. Duan, W. P. Cai, *J. Am. Ceram. Soc.* **2014**, *97*, 2177.
[15] B. Q. Cao, T. Matsumoto, M. Matsumoto, M. Higashihata, D. Nakamura, T. Okada, *J. Phys. Chem. C* **2009**, *113*, 10975.
[16] G. W. Yang, *Prog. Mater. Sci.* **2007**, *52*, 648.
[17] C. H. Liang, S. Yoshiki, M. Mitsutoshi, S. Takeshi, K. Naoto, *Chem. Mater.* **2004**, *16*, 963.
[18] X. L. Hu, H. B. Gong, H. Y. Xu, H. M. Wei, G. Q. Liu, H. B. Zeng, W. P. Cai, B. Q. Cao, *J. Am. Ceram. Soc.* **2011**, *94*, 4305.
[19] S. Noël, J. Hermann, T. Itina, *Appl. Surf. Sci.* **2007**, *253*, 6310.
[20] S. K. Yang, W. P. Cai, H. W. Zhang, X. X. Xu, H. B. Zeng, *J. Phys. Chem. C* **2009**, *113*, 19091.
[21] S. Link, C. Burda, B. Nikoobakht, M. A. El-Sayed, *J. Phys. Chem. B* **2000**, *104*, 6152.
[22] H. Q. Wang, N. Koshizaki, L. Li, L. C. Jia, K. Kawaguchi, X. Y. Li, A. Pyatenko, Z. S. Warkocka, Y. Bando, D. Golberg, *Adv. Mater.* **2011**, *23*, 1865.
[23] X. L. Hu, H. B. Gong, Y. G. Wang, Q. Chen, J. Zhang, S. H. Zheng, S. K. Yang, B. Q. Cao, *J. Mater. Chem.* **2012**, *22*, 15947.
[24] X. Y. Song, Z. W. Qiu, X. P. Yang, H. B. Gong, S. H. Zheng, B. Q. Cao, H. Q. Wang, H. Möhwald, D. Shchukin, *Chem. Mater.* **2014**, *26*, 5113.
[25] D. Kim, H. J. Lee, *J. Appl. Phys.* **2001**, *89*, 5703.
[26] L. B. Wang, W. M. Liu, X. B. Wang, *Tribol. Lett.* **2010**, *37*, 381.
[27] D. Jiao, S. H. Zheng, Y. Z. Wang, R. F. Guan, B. Q. Cao, *Appl. Surf. Sci.* **2011**, *257*, 5720.
[28] X. D. Zhou, D. M. Wu, H. Q. Shi, X. Fu, Z. S. Hu, X. B. Wang, F. Y. Yan, *Tribol. Int.* **2007**, *40*, 863.
[29] N. V. Brilliantov, T. Pöschel, *Europhys. Lett.* **1998**, *42*, 511.
[30] D. X. Peng, Y. Kang, R. M. Hwang, S. S. Shyr, Y. P. Chang, *Tribol. Int.* **2009**, *42*, 911.

[31] C. Drummond, N. Alcantar, J. Israelachvili, R. Tenne, Y. Golan, *Adv. Funct. Mater.* **2001**, *11*, 348.
[32] H. Kato, K. Komai, *Wear* **2007**, *262*, 36.
[33] L. L. Zhang, J. P. Tu, H. M. Wu, Y. Z. Yang, *Mater. Sci. Eng. A* **2007**, *454*, 487.
[34] G. Liu, X. Li, B. Qin, D. Xing, Y. Guo, R. Fan, *Tribol. Lett.* **2004**, *17*, 961.
[35] W. Li, S. H. Zheng, B. Q. Cao, S. Y. Ma, *J. Nanopart. Res.* **2011**, *13*, 2129.
[36] X. Y. Song, S. H. Zheng, J. Zhang, W. Li, Q. Chen, B. Q. Cao, *Mater. Res. Bull.* **2012**, *27*, 4305.
[37] W. Li, S. H. Zheng, Q. Chen, B. Q. Cao, *Mater. Chem. Phys.* **2012**, *134*, 38.
[38] Q. Chen, S. H. Zheng, S. K. Yang, W. Li, X. Y. Song, B. Q. Cao, *J. Sol-Gel Sci. Technol.* **2012**, *61*, 501.
[39] H. B. Qiao, Q. Guo, A. G. Tian, G. L. Pan, L. B. Xu, *Tribol. Int.* **2007**, *40*, 105.
[40] S. Radice, S. Mischler, *Wear* **2006**, *261*, 1032.

